Axial Loading Behavior of CFRP Strengthened Concrete-Filled Steel Tubular Stub Columns

Zhong Tao[1,*], Lin-Hai Han[2,3] and Jin-Ping Zhuang[1]

[1]College of Civil Engineering, Fuzhou University,
Gongye Road 523, Fuzhou, Fujian Province, 350002, People's Republic of China
[2]Department of Civil Engineering, Tsinghua University, Beijing, 100084, People's Republic of China
[3]Key Laboratory of Structural Engineering and Vibration of China Education Ministry, Beijing, 100084, People's Republic of China

(Received: 13 August 2005; Received revised form: 18 April 2006; Accepted: 2 August 2006)

Abstract: This paper presents the axial compression test results of concrete-filled steel tubular (CFST) stub columns strengthened with carbon fiber reinforced polymer (CFRP) composites. Both circular and rectangular specimens were tested to investigate the retrofitting effects of CFRP composites on them. The test results showed that the CFRP jackets enhanced the load bearing capacity of the circular columns effectively, whereas the enhancement was not so significant for rectangular columns. However, ductility was enhanced to some extent for those rectangular columns. A simple model is proposed to calculate the ultimate strength of circular CFST stub columns wrapped with CFRP. The predicted results are generally in good agreement with the experimental ones obtained in this study and in the literature.

Key words: concrete-filled steel tubes (CFST), hybrid columns, fiber reinforced polymers (FRP), hollow section, stub column, strengthening, confinement.

1. INTRODUCTION

The use of concrete-filled steel tubes (CFST) in different areas of construction has increased in recent years, especially in tall buildings and arch bridges (Tao and Han 2006). The composite columns combine the advantages of both steel and concrete. It provides not only an increase in the load carrying capacity but also economy and rapid construction, and thus additional cost saving.

With the increasing use of CFST in practice, the risk of fire is high, especially in high-rise buildings. Therefore, there is a need to study the residual strength and possible retrofit measures to enhance strength and/or ductility of the composite columns (Han and Huo 2003). Furthermore, strengthening may also be arisen if changes in the use of the structures imposing higher functional requirements than those anticipated in the original design are to take place.

Fiber reinforced polymer (FRP) composites have found increasingly wide applications in civil engineering, characterized by high strength-to-weight ratio and high corrosion resistance. Therefore, many researches have been undertaken using this new material to retrofit reinforced concrete structures or steel structures (Holloway and Leeming 1999; Teng *et al*. 2002; Lam and Clark 2003; Jiao and Zhao 2004). One of the research focuses is on the behavior and modeling of FRP-confined concrete. Detailed review of existing work on FRP-confined concrete can be found in Teng *et al*. (2002) and Teng and Lam (2004).

So far, there has been very little study on the retrofit of CFST columns (Gu *et al*. 2004; Xiao 2004; Xiao *et al*. 2005). Gu *et al*. (2004) tested 12 CFST stub columns with circular steel tube shapes. Eight of them were strengthened with CFRP composites. Xiao *et al*. (2005)

*Correspondence author. Email address: taozhong@fzu.edu.cn; Fax: +86-591-8373-7442; Tel: +86-591-8370-3490.

proposed a new CFST column system, where CFRP composites were used as additional confinement to the potential plastic hinge regions of the composite column. Test results on eight CFRP strengthened circular CFST stub columns and one companion CFST specimen were reported. Testing parameters were the number of layers of CFRP wraps and with or without a gap between the steel tube. The gap was so designed to delay the participation of the CFRP wraps for maximizing the deformability while minimizing the unnecessary strength enhancement. The test results reported by Gu *et al*. (2004) and Xiao *et al*. (2005) have preliminarily demonstrated the effectiveness of the CFRP wraps in increasing the axial loading capacity of CFST columns. However, no research has been conducted on CFST specimens with non-circular CFST sections, and it seems more research is needed to understand the composite action between the CFRP wraps and the composite columns.

In this study, experimental results obtained from the CFST stub columns are presented. Both circular and rectangular specimens, as shown in Figure 1, were tested to investigate the retrofitting effects of CFRP composites on them. Two CFRP-confined concrete cylinders were also tested to provide the benchmark behavior data, with one and two plies of CFRP wraps outside respectively. A simple model is proposed to calculate the ultimate strength of CFRP wrapped circular CFST stub columns.

2. OUTLINE OF EXPERIMENT

2.1. General

A total of nine CFST specimens were prepared and tested. Six of them were with circular cross-sections, and three of them were with rectangular cross-sections. The specimens can be classified as three categories: columns without CFRP confinement, columns strengthened with only one ply of CFRP, and columns strengthened with two plies of CFRP. CFRP strengthening was achieved by the external wrapping of unidirectional carbon fiber sheets with the fibers oriented in the hoop direction of the columns. Table 1 provides a summary of the specimens, in which t_s is the thickness of the steel tube and t_{frp} the nominal thickness of the CFRP jacket. In addition, two concrete cylinders were also prepared and tested for

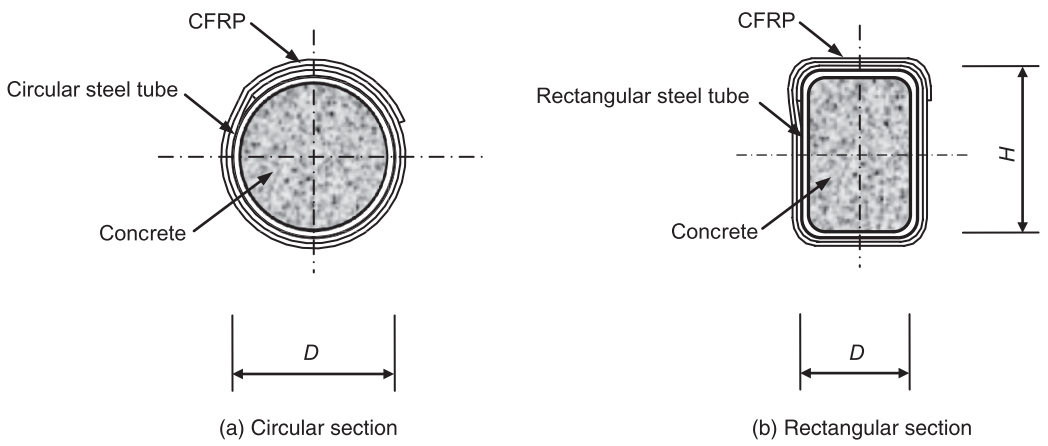

Figure 1. Cross-sections of CFRP strengthened concrete-filled steel tubes

Table 1. Specimen labels and member capacities of CFST stub columns

Specimen label	Section dimensions	L (mm)	t_s (mm)	Layer(s) of CFRP	t_{frp} (mm)	ξ_s	ξ_{frp}	N_{ue} (kN)	SEI	N_{uc} (kN)	N_{uc}/N_{ue}
C1-0	ϕ156	470	3.0	0	0	0.408	0	1540	—	1245	0.809
C1-1	ϕ156	470	3.0	1	0.17	0.408	0.432	1890	22.7%	1649	0.873
C1-2	ϕ156	470	3.0	2	0.34	0.408	0.865	2270	47.4%	2053	0.905
C2-0	ϕ250	750	3.0	0	0	0.249	0	3285	—	2831	0.862
C2-1	ϕ250	750	3.0	1	0.17	0.249	0.262	3940	19.9%	3478	0.883
C2-2	ϕ250	750	3.0	2	0.34	0.249	0.524	4780	45.5%	4126	0.863
R-0	100×150	450	3.2	0	0	0.906	0	1185	—	—	—
R-1	100×150	450	3.2	1	0.17	0.906	0.548	1285	8.4%	—	—
R-2	100×150	450	3.2	2	0.34	0.906	1.095	1280	8.0%	—	—

comparison, with one and two plies of CFRP wraps outside, respectively. The length of the CFST specimens (L) was chosen to be three times the diameter of a circular section or three times the height of the rectangular section.

2.2. Material Properties

Tensile tests on steel coupons cut from the same original steel tube were conducted. The measured properties of the steel tubes from tests are given in Table 2.

The tensile properties of the cured CFRP determined from tensile tests of flat coupons according to ASTM D3039 (2000) are given in Table 3, where the values presented are the averages from five test coupons calculated on the basis of the nominal thickness of 0.17 mm for the fiber sheet. The tensile properties of the epoxy as provided by the supplier are also given in Table 3.

All the specimens were cast with one batch of concrete. Maximum size of coarse aggregate is 20 mm. To determine the compressive strength of concrete, six 150 mm cubes and three standard cylinders (150 mm× 300 mm) were cast and cured in conditions similar to the related specimens. The average cube strength (f_{cu}) and the average modulus of elasticity (E_c) at 28 days were 47.8 N/mm^2 and 30,800 N/mm^2 respectively, whilst those at the time of tests were found to be 57.8 N/mm^2 and 35,800 N/mm^2 respectively. The average cylinder strength (f_c') at the time of tests was 46 N/mm^2.

2.3. Preparation of Specimens

In preparing the CFST columns, the concrete was filled in layers and was vibrated by a poker vibrator. These specimens were then placed upright to air-dry until testing. Prior to testing, the top surfaces of the CFST specimens were ground smooth and flat using a grinding wheel with diamond cutters. A steel plate with a thickness of 12mm was then welded to the top of each of those specimens. All of the tested cylinders were capped before testing using a sulfur mortar capping compound.

Carbon fiber sheets were applied using a hand lay-up method after the concrete had been cured for 28 days. The finishing end of a sheet overlapped the starting end by 150 mm. The wrapped specimens were left to cure in the laboratory environment at room temperature for about one month before testing.

2.4. Test Setup and Instrumentation

A 5,000 kN capacity testing machine was used for the compression tests of all specimens. Eight strain gauges, including four in the axial direction and another four in the transverse direction, mounted on the surface of the specimen, were used for each specimen to measure strains at the mid-height. Eight additional strain gauges were attached to the steel tube surface for some of the CFRP strengthened specimens. Comparison of strains in the steel tube and those in the CFRP jacket in close proximity allowed slip to be readily detected. Two linear variable displacement transducers (LVDTs) were used to measure the axial shortening during the tests. A computerized IMP data acquisition system was used for data logging. The axial compression test setup is shown in Figure 2. To assure uniform compression, preliminary test within the elastic range were conducted by carefully adjusting the position of the specimen, based on the measurements of strain gauges attached at the mid-height of the test specimen. The adjustment was terminated until the difference between the measured strain and the average value was no more than 5%. A load interval of less than one tenth of the estimated load capacity was used. Each load interval was maintained for about 2 to 3 minutes.

3. EXPERIMENTAL RESULTS AND DISCUSSIONS

Figure 3 compares the axial and lateral strains of typical CFRP strengthened circular and rectangular CFST specimens, which measured from strain gauges mounted

Table 2. Material properties of steel

Steel thickness (mm)	Elastic modulus (GPa)	Yield strength (MPa)	Yield strain ($\times 10^{-6}$)	Ultimate strength (MPa)	Ultimate strain (%)
3.0	206	230	3036	337	40.5
3.2	209	380	3820	476	25.1

Table 3. Material properties of CFRP and epoxy

Material	Elastic modulus (GPa)	Tensile strength (MPa)	Ultimate strain (%)	Thickness (mm)
CFRP	255	4,212	1.67	0.170 (nominal)
Epoxy	2.8	48.3	3.1	—

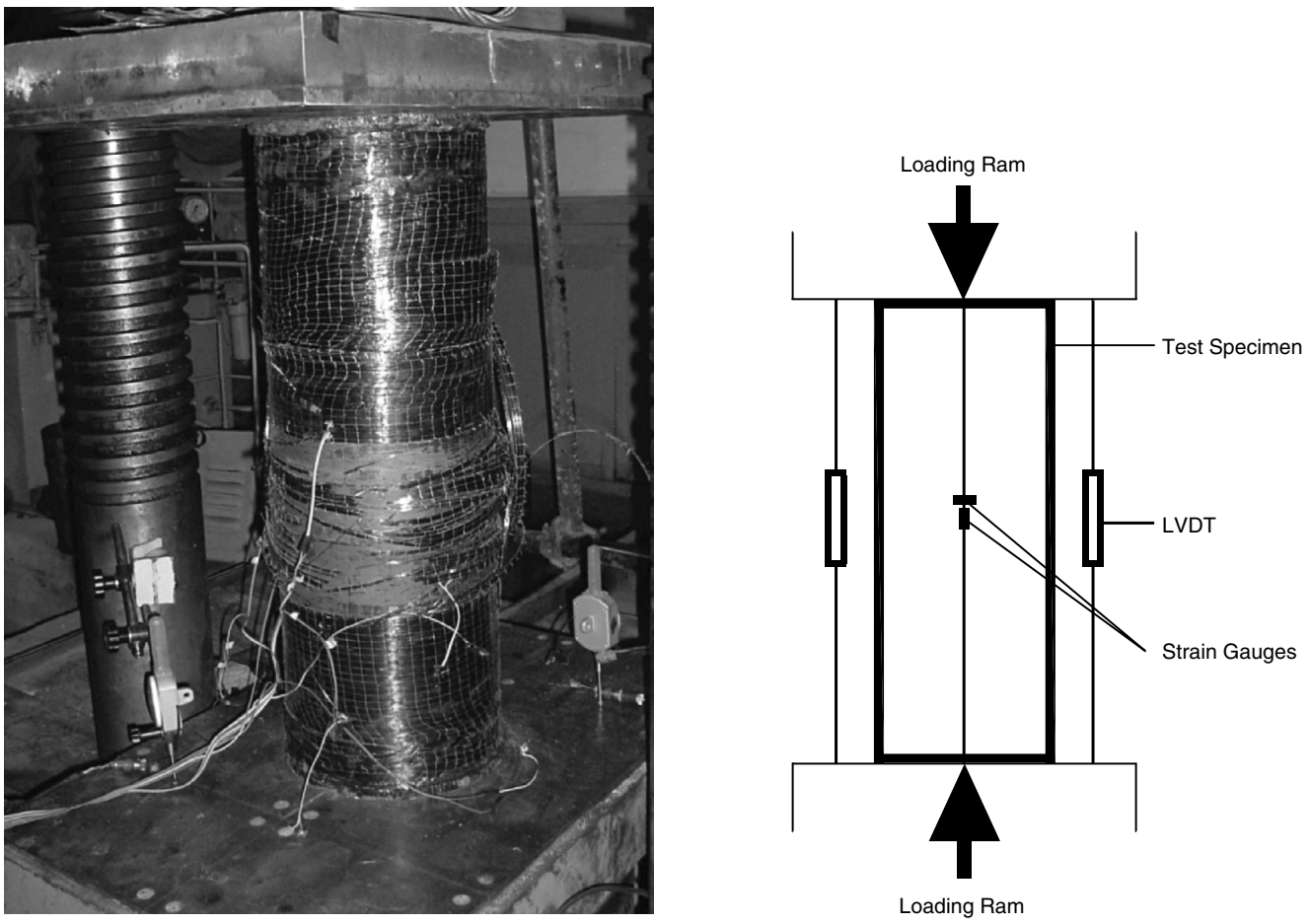

Figure 2. Axial compression test setup

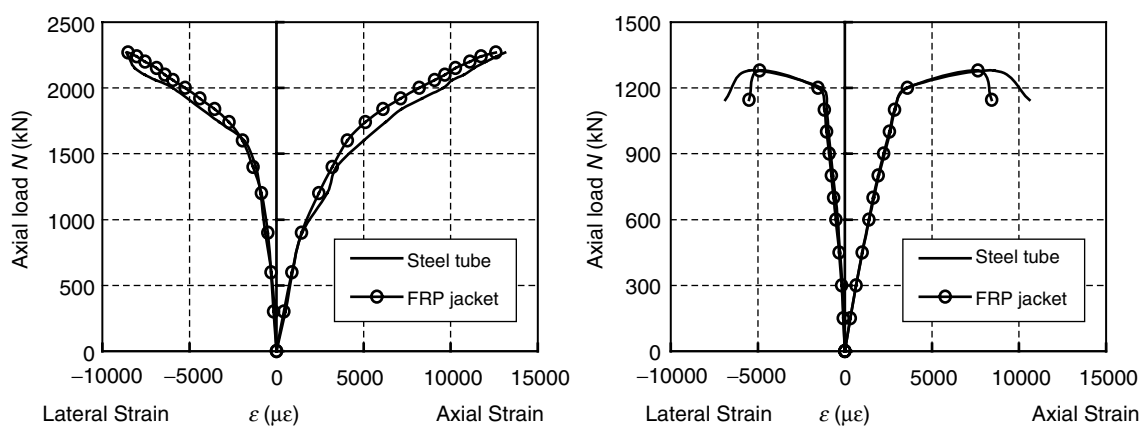

(a) Specimen C1-2 with circular section (b) Specimen R-2 with rectangular section

Figure 3. Comparison between measured strains of the steel tubes and the FRP jackets

on the surfaces of the steel tubes and the CFRP jackets. It can be seen that, for a wrapped CFST column, the development of both axial and lateral strains of the steel tube is almost the same as that of its CFRP jacket until the jacket ruptured. It means that the slip between the tube and the jacket was negligible, and the two components worked well together before the jacket failed. Therefore, only strains measured from strain gauges mounted on the specimen surfaces were used to plot the load versus strain curves. LVDTs were used to

measure the axial strain of the specimen after the rupture of the jacket, so that the behavior of the test specimen can be evaluated when the jacket failed. The tested curves of load versus axial and lateral strains are shown in Figure 4. It can be seen that, the initial portion of load-strain responses of a confined CFST column essentially followed the curve of its corresponding unconfined column before attaining a characteristic strain. The characteristic strain for specimens of series C2 or R is near the peak point of corresponding unconfined specimen, and that for specimens of series C1 is the point when achieved 80 percent of peak load of specimen C1-0. It seems that the steel tubes of series C1 could exert higher confinement on the concrete cores, thus have larger elastic-plastic deformations. After attaining the characteristic strain, the load-axial strain and load-lateral strain relationships of confined specimens show a higher modulus than those of the companion unconfined specimen, and eventually exhibited an almost linear behavior until the sudden failure due to the rupture of the CFRP jackets at the midheight. For the rectangular specimens, the rupture of the CFRP jackets occurred at the corners.

Figure 5 shows the effect of CFRP confinement on the axial strain at peak load ε_{cc}. It can be seen from Figure 5 that the value of ε_{cc} measured in a wrapped CFST specimen is larger than that of its unwrapped counterpart. Generally, the ultimate strain at the peak load increases with the increasing number of CFRP layers.

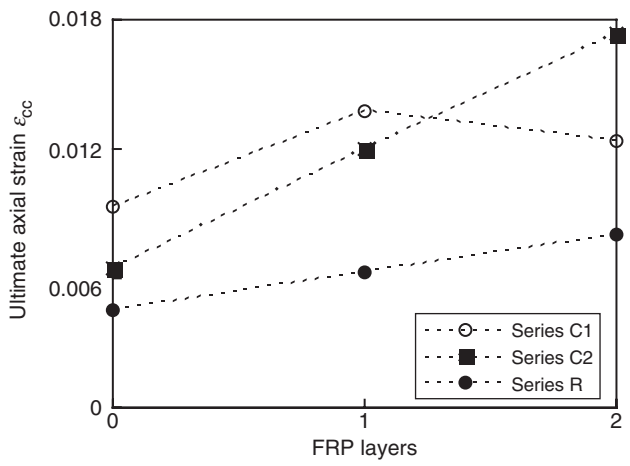

Figure 5. Effect of FRP jacket on ultimate axial strain ε_{cc}

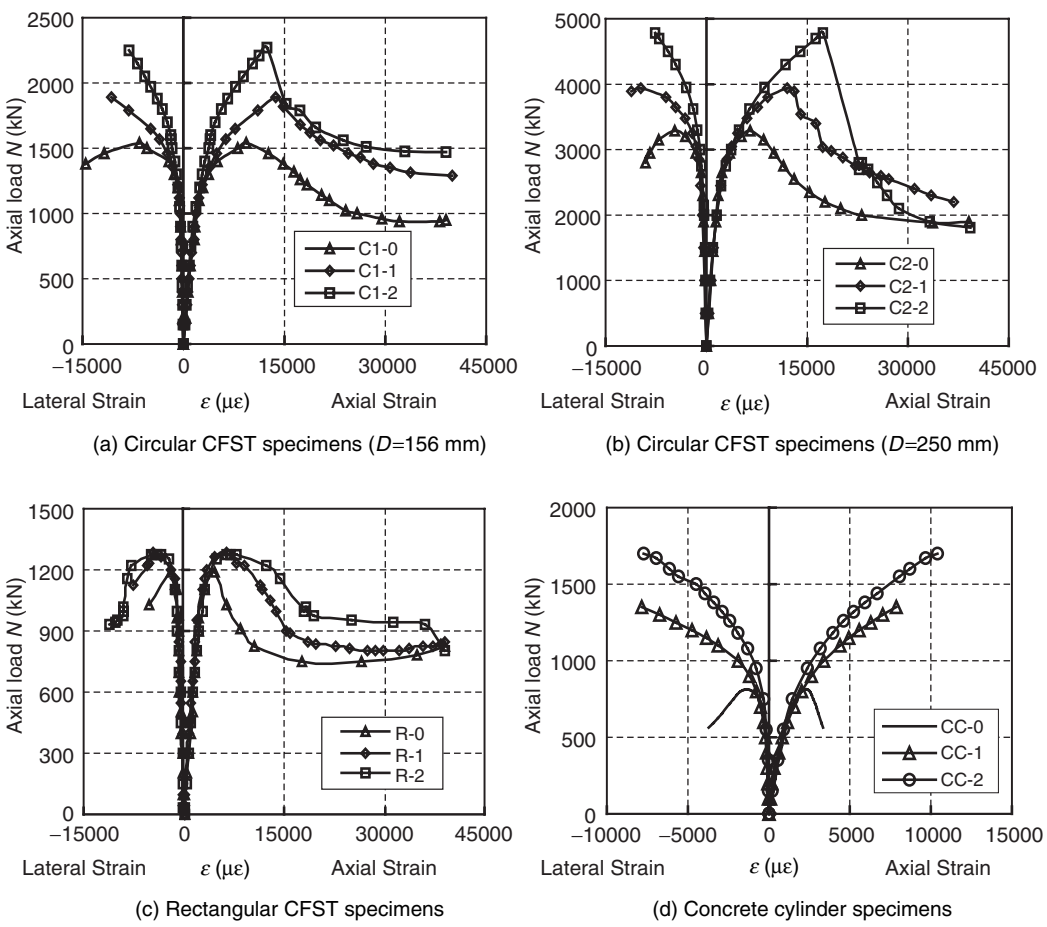

Figure 4. Load versus strain curves for tested specimens

All CFST specimens exhibited a descending response. In the test program, it was observed that the rectangular steel tubes buckled earlier than the rupture of the CFRP jackets, while for the circular steel tubes it was the opposite. All strengthened steel tubes buckled later than the un-strengthened ones.

Generally, during the post-peak stage, CFRP-wrapped specimen had higher residual strength compared with its unwrapped counterpart. It seems the CFRP jacket still had some effects on the residual strength of a wrapped specimen.

Figure 6 shows all wrapped and unwrapped specimens after testing. Figure 7 shows typical failure appearances of the steel tubes for specimens of series C2.

In order to quantify the effect of CFRP jackets on section ductility, a ductility index (*DI*) is defined in this paper as

$$DI = \frac{\varepsilon_{85\%}}{\varepsilon_{y}} \tag{1}$$

where $\varepsilon_{85\%}$ is the axial strain when the load falls to 85% of the ultimate load, and ε_y is equal to $\varepsilon_{75\%}$ /0.75, $\varepsilon_{75\%}$ is the axial strain when the load attains of 75% the ultimate load in the pre-peak stage, shown in Figure 8.

The ductility indexes (*DI*) so determined are plotted in Figure 9 against the numbers of CFRP layers. It can be seen from Figure 9 that the ductility of the strengthened circular specimens decreases with the increasing number of CFRP layers, whereas that for strengthened rectangular specimens is the opposite. The reason may be attributed to the fact, that the rupture of the CFRP jackets of rectangular specimens was induced from the local buckling of the tubes. The rupture process was much slower than that of jackets in circular shapes. The more abrupt rupture of the CFRP jackets of circular specimens was due to hoop tension, with a lateral rupture strain approximately equal to that in the corresponding concrete cylinder specimen.

Two plain concrete cylinders (150 mm × 300 mm) were also prepared and tested for comparison, which

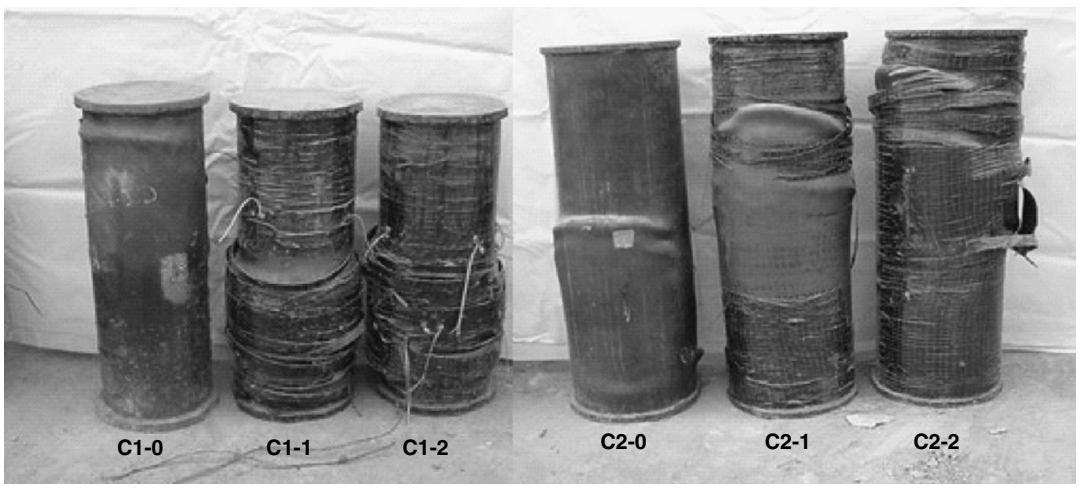

(a) Circular CFST

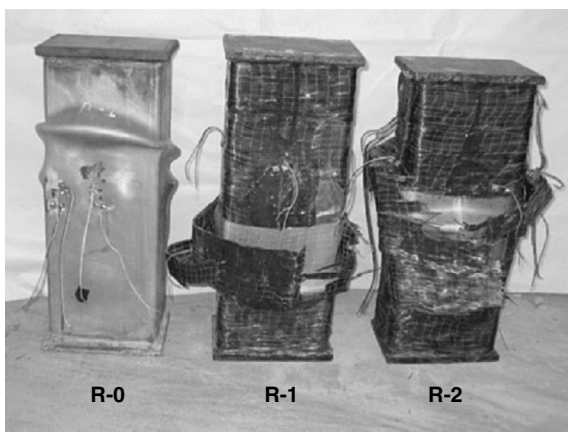

(b) Rectangular CFST

(c) Plain concrete cylinders

Figure 6. Specimens after testing

Figure 7. Typical failure appearances of the steel tubes after removal of the FRP jackets

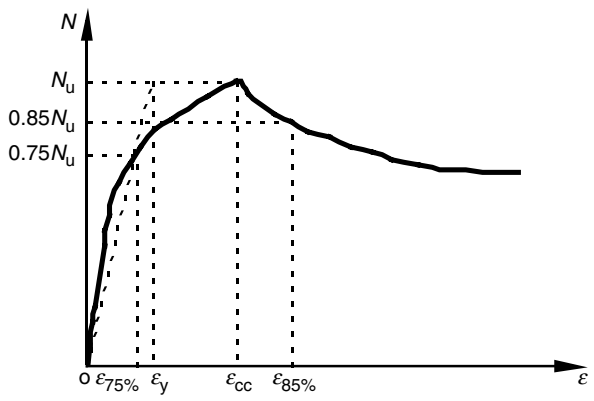

Figure 8. Definition of the ductility index

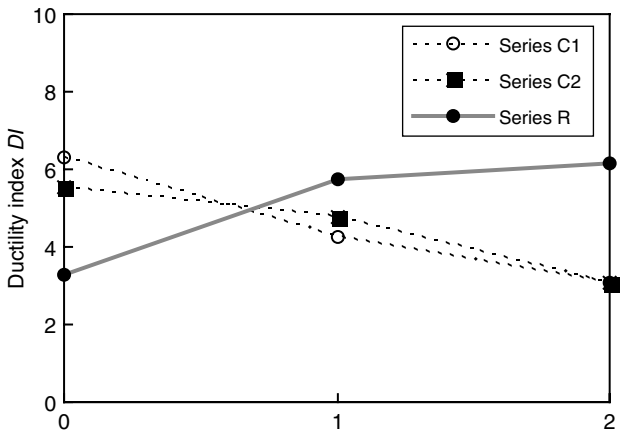

Figure 9. Effect of FRP confinement on ductility

were wrapped with one or two plies of CFRP outside, respectively. According to the plies of CFRP wrapped, the cylinders were labelled as CC-1 and CC-2 respectively. They had a same cross-sectional area as that of the concrete fillings in CFST specimens of series C1.

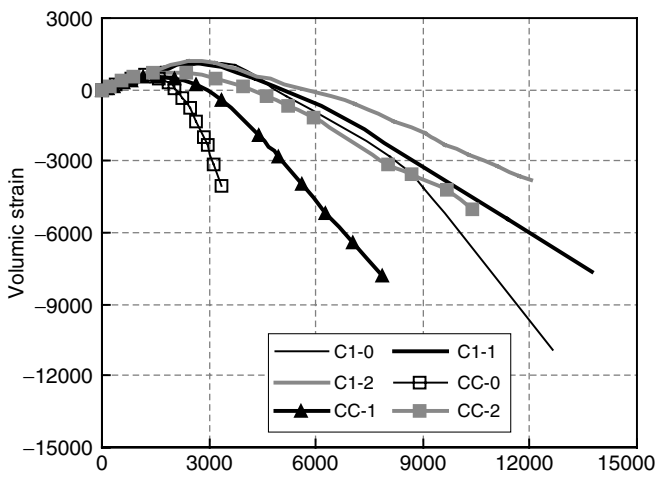

Figure 10. Volumetric responses of concrete with a same diameter of 150 mm

The confined concrete showed eventual failure by the sudden rupture of the CFRP jackets (see Figure 6 (c)). The measured peak loads for unconfined concrete cylinders (labeled as CC-0) and cylinders of CC-1 and CC-2 are 813kN, 1350kN and 1700kN respectively.

Figure 10 illustrates the tested volumetric changes of concrete with a same diameter of 150 mm. A positive volumetric strain indicates compaction while a negative value corresponds to dilation. As expected, the volumetric strain for all specimens changes from compaction to unstable dilation. It is interesting to note that the volumetric changes of the CFRP strengthened CFST columns essentially followed the curves of unconfined CFST columns in the compaction stage. However, in the dilation stage, the dilation ratio decreased with the increasing number of CFRP layers. This is attributed to the confinement from the CFRP jackets.

The maximum loads (N_{ue}) obtained in the test are summarized in Table 1. Enhancements in the axial load capacity of wrapped CFST columns due to CFRP wrapping can be easily gauged using the strengthening ratio defined as the percentage increase in the ultimate load:

$$SEI = (N_{eS} - N_{eU})/N_{eU} \quad (2)$$

where N_{eS} and N_{eU} are maximum loads for wrapped and unwrapped specimens. The values of *SEI* are shown in Table 1. Figure 11 shows the effect of CFRP confinement on *SEI*. It can be seen from Figure 11 and Table 1 that the load-carrying capacity of CFRP strengthened circular CFST columns increases with the increasing number of CFRP layers. However, the

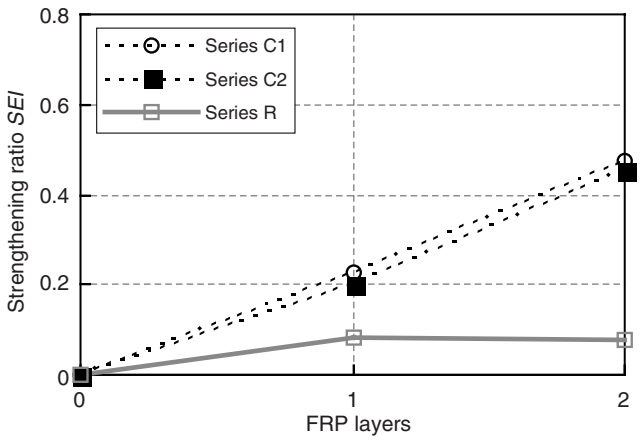

Figure 11. Effect of FRP confinement on strengthening ratio

enhancement was not so significant for rectangular columns compared with their circular counterparts. Rectangular column wrapped with two layers of CFRP jackets has almost a same peak load compared with the specimen wrapped with only one layer of CFRP jacket.

Based on the test results of plain concrete cylinders and specimens of series C1, the mutual influence of dual confining system of CFRP and steel tube can be evaluated. It is assumed that the enhancement of bearing-capacity in CFRP strengthened CFST column comes from a joint confinement of steel tube ($N_{c,s}$) and CFRP ($N_{c,frp}$). Therefore, $N_{c,s}$ is calculated by

$$N_{c,s} = N_{ue} - N_s - (N_c + N_{c,frp}) \tag{3}$$

where N_{ue} is measured peak load of CFRP strengthened CFST column, N_s and N_c are axial loads carried by the steel tube and the concrete respectively, without considering the mutual action between the CFRP jacket and the CFST column. In Eqn 3 the term of N_c+$N_{c,frp}$ can be determined by measured peak load of plain concrete cylinders, and the term of N_s is determined by $A_s f_y$. The calculated values of $N_{c,s}$ are listed in Table 4.

From Table 4, it seems that the steel tube has less confinement on concrete in wrapped CFST column compared with its unwrapped counterpart in the current test. The reason is attributed to the fact that the volume dilation rate is slower under the dual confining system than that of concrete confined only by a steel tube.

4. LOAD-CARRYING CAPACITY PREDICTION

Since the CFRP confinement has no significant effect on ultimate capacity of rectangular CFST columns in the current test, calculation method is discussed only for CFRP strengthened circular CFST columns. According to research results reported by Han (2004) for CFST column and Yu (2002) for CFRP-confined concrete, the "composite action" between the steel tube and the concrete core or the CFRP jacket and the concrete core can be described by confinement factors of ξ_s and ξ_{frp} respectively. They are expressed as:

$$\text{For CFST:} \qquad \xi_s = A_s f_y / A_c f_c' \tag{4}$$

$$\text{For CFRP-confined concrete:} \quad \xi_{frp} = A_{frp} f_{frp} / A_c f_c' \tag{5}$$

where A_s, A_{frp} and A_c are the cross-sectional areas of the steel tube, the CFRP jacket and the concrete respectively. The higher is the confinement factor, the more effective the confinement on the concrete core.

For circular CFST stub column, the following formula was put forward by Han *et al*. (2004) to calculate its section capacity:

$$N_u = (1.14 + 1.02\xi) f_{ck} A_{sc} \tag{6}$$

in which $\xi = A_s f_y / A_c f_{ck}$, f_{ck} (=$0.67 f_{cu}$) is characteristic concrete strength.

For CFRP-confined concrete, its ultimate strength can be calculated by (Yu 2002):

$$N_u = (1 + 1.15\xi_{frp}) f_c' A_c \tag{7}$$

As can be seen, both Eqn 6 and Eqn 7 are quite simple. However, the accuracy of them has been confirmed by extensive test results, and they have good accuracy compared with other existing formulas (Teng *et al*. 2002; Yu 2002; Han 2004).

Based on Eqn 6 and Eqn 7, the following formula is proposed in this paper:

$$N_u = (1 + 1.02\xi_s) f_c' A_{sc} + 1.15\xi_{frp} f_c' A_c \tag{8}$$

Table 4. Contributions of different components to bearing capacities for specimens of series C1

Specimen label	D (mm)	t_s (mm)	f_y (MPa)	Layer(s) of CFRP	t_{frp} (mm)	N_{ue} (kN)	N_s (kN)	N_c+$N_{c,frp}$ (kN)	$N_{c,s}$ (kN)
C1-0	156	3.0	230	0	0	1540	332	813	395
C1-1	156	3.0	230	1	0.17	1890	332	1350	208
C1-2	156	3.0	230	2	0.34	2270	332	1700	238

Table 5. Comparisons of experimental and predicted ultimate strengths for specimens from independent experiments

Specimen label	D (mm)	t_s (mm)	f_y (MPa)	f_{cu} (MPa)	f'_c (MPa)	Layer(s) of CFRP	t_{frp} (mm)	f_{frp} (MPa)	ξ_s	ξ_{frp}	N_{ue} (kN)	N_{uc} (kN)	N_{uc}/N_{ue}
Gu *et al*. (2004)													
0-1.5	127	1.5	350	55	—	0	0	—	0.465	—	889.8	830	0.903
0-2.5	129	2.5	350	55	—	0	0	—	0.781	—	1139.7	1050	0.864
0-3.5	131	3.5	310	55	—	0	0	—	0.977	—	1292.6	1207	0.862
0-4.5	133	4.5	310	55	—	0	0	—	1.265	—	1527.8	1432	0.851
1-1.5	127	1.5	350	55	—	1	0.167	1260	0.465	0.189	1085.8	901	0.830
1-2.5	129	2.5	350	55	—	1	0.167	1260	0.781	0.192	1293.6	1083	0.837
1-3.5	131	3.5	310	55	—	1	0.167	1260	0.977	0.195	1347.5	1214	0.901
1-4.5	133	4.5	310	55	—	1	0.167	1260	1.265	0.198	1689.3	1401	0.829
2-1.5	127	1.5	350	55	—	2	0.334	1260	0.465	0.378	1282.8	998	0.778
2-2.5	129	2.5	350	55	—	2	0.334	1260	0.781	0.384	1506.3	1181	0.785
2-3.5	131	3.5	310	55	—	2	0.334	1260	0.977	0.390	1592.5	1314	0.825
2-4.5	133	4.5	310	55	—	2	0.334	1260	1.265	0.396	1846.3	1502	0.814
Xiao *et al*. (2005)													
CFT	152	2.95	356	—	46.6	0	0	0	0.629	0	1453	1389	0.956
CCFT-2L-1	152	2.95	356	—	46.6	2	2.8	897	0.629	1.563	2233	2793	1.251
CCFT-2L-2	152	2.95	356	—	46.6	2	2.8	897	0.629	1.563	2266	2793	1.233
CCFT-4L-1	152	2.95	356	—	46.6	4	5.6	897	0.629	3.184	3439	4249	1.235
CCFT-4L-2	152	2.95	356	—	46.6	4	5.6	897	0.629	3.184	3438	4249	1.236

The predicted ultimate loads (N_{uc}) using Eqn 8 are compared with the experimental values (N_{ue}) obtained in this paper. The comparisons are shown in Table 1. A mean ratio (N_{uc}/N_{ue}) of 0.849 is obtained with a COV (coefficient of variation) of 0.037. In general, the predictions are reasonable and somewhat conservative.

Eqn 8 is also used to analyze the test results presented in Gu *et al*. (2004) and Xiao *et al*. (2005). The comparisons are shown in Table 5. As can be seen, the predictions are reasonable and conservative for the tests reported in Gu *et al*. (2004). However, the predictions are generally higher than the experimental results reported in Xiao *et al*. (2005). The reason may be attributed to the fact that these specimens have comparatively high values of ξ_{frp}. It seems more research should be carried out when strong confinement is exerted on CFST columns.

5. CONCLUSIONS

The main conclusions obtained by this study can be summarized as follows:

1) Similar to CFRP-confined concrete, sectional shape has significant influence on the confining effect of CFRP jackets exerted on CFST columns. CFRP jackets can enhance the load bearing capacity of the circular CFST columns effectively, whereas the enhancement is not so significant for rectangular CFST columns.
2) The load-carrying capacity of CFRP strengthened circular CFST columns increase with the increasing number of CFRP layers. However, this phenomenon was not evident for rectangular CFST columns in the current test.
3) The ductility of the strengthened circular specimens decreases with the increasing number of CFRP layers, whereas that for strengthened rectangular specimens is to the contrary.
4) Generally, during the post-peak stage, CFRP-wrapped specimen has higher residual strength compared with its unwrapped counterpart.
5) A simple formula is proposed for predicting bearing-capacity of CFRP strengthened circular CFST stub columns. In general, the predictions are reasonable when the CFRP confinement is not too strong.

ACKNOWLEDGEMENTS

The research reported in the paper was supported by the National Natural Science Foundation of China (No.50425823 and No.50608019), the Start-Up Fund for Outstanding Incoming Researchers Project of Fujian Province, the Key Grant of Chinese Ministry of Education (No. 205083), and the Foundation of Science and Technology Department of Fujian Province (E0410015). The financial support is highly appreciated.

REFERENCES

ASTM D3039/D3039M (2000). *Standard Test Method for Tensile Properties of Polymer Matrix Composite Material*, Annual book of ASTM Standards, American Society for Testing and Materials, West Conshohocken, PA.

Gu, W., Guan, C.W., Zhao, Y.H. and Cao, H. (2004). "Experimental study on concentrically-compressed circular concrete filled CFRP-steel composite tubular short columns", *Journal of Shenyang Architectural and Civil Engineering University (Natural Science)*, Vol. 20, No. 2, pp. 118–120 (in Chinese).

Han, L.H. and Huo, J.S. (2003). "Concrete-filled hollow structural steel columns after exposure to ISO-834 fire standard", *Journal of Structural Engineering,* ASCE, Vol. 129, No. 1, pp. 68–78.

Han, L.H., Yao, G.H. and Zhao, X.L. (2004). "Behavior and calculation on concrete-filled steel CHS (Circular Hollow Section) beam-columns", *Steel and Composite Structures*, Vol. 4, No. 3, pp. 169–188.

Holloway, L.C., Leeming, M.B. (1999). *Strengthening of Reinforced Concrete Structures: Using Externally-Bonded FRP Composites in Structural and Civil Engineering*, Woodhead Publishing Limited, Cambridge.

Jiao, H. and Zhao, X.L. (2004). "CFRP strengthened butt-welded very high strength (VHS) circular steel tubes", *Thin-Walled Structures*, Vol. 42, No. 7, pp. 963–978.

Lam, D. and Clark, K.A. (2003). "Strengthening steel sections using carbon fibre reinforced polymers laminates", *Proceedings of the International Conference on Advances in Structures*, Sydney, Australia, June, pp. 1369–1374.

Tao, Z. and Han, L.H. (2006). "Behaviour of concrete-filled double skin rectangular steel tubular beam-columns", *Journal of Constructional Steel Research*, Vol. 62, No. 7, pp. 631–646.

Teng, J.G., Chen, J.F., Smith, S.T. and Lam, L. (2002). *FRP-Strengthened RC Structures*, John Wiley & Sons, Ltd..

Teng, J.G. and Lam, L. (2004). "Behavior and modeling of fiber reinforced polymer-confined concrete", *Journal of Structural Engineering*, ASCE, Vol. 130, No. 11, pp. 1713–1723

Xiao, Y. (2004). "Applications of FRP composites in concrete columns", *Advances in Structural Engineering*, Vol. 7, No. 4, pp. 335–343.

Xiao, Y., He, W.H. and Choi, K.K. (2005). "Confined concrete-filled tubular columns", *Journal of Structural Engineering*, ASCE, Vol. 131, No. 3, pp. 488–497.

Yu, Q. (2002), *Behaviors of FRP-Confined Concrete Columns*. Dissertation for the Master Degree in Engineering, Harbin Institute of Technology (in Chinese).